Mechanics & Industry **20**, 503 (2019)
© AFM, EDP Sciences 2019
https://doi.org/10.1051/meca/2019024

Mechanics & Industry

Available online at:
www.mechanics-industry.org

Regular Article

# A modeling study on the effect of operating parameters on RHCM process using split flow channels design

Fatma Kria*, Moez Hammami, and Mounir Baccar

Mechanical Engineering department, National Engineering School of Sfax, Sfax, Tunisia

Received: 18 December 2017 / Accepted: 22 March 2019

**Abstract.** In this work, a three-dimensional numerical study of thermal behavior of RHCM mold for automotive parts production was undertaken. Particularly, simulation of several heating/cooling cycles was conducted to determine, at the regular cyclic regime, thermal behaviors at cavity/core plates and polymer as well as thermal and hydrodynamic behaviors at cooling water. It was demonstrated that heating/cooling channels with split flow design are suitable for RHCM regulation. Besides, to further promote part quality, process productivity, and profitability, the effect of cooling parameters, such as the coolant temperature and flow velocity in channels, on the RHCM process efficiency was analyzed. To highlight the influence of these parameters on the productivity and profitability of the process, the cycle time and the consumed energy were used. Temperature gap at the cavity plate surfaces after the heating phase as well as the maximum temperature difference (MTD) in the polymer part after the cooling phase were used as criteria to evaluate the automotive part quality. The results show that the coolant temperature increase in the range between 30 and 60 °C reduces the energy consumption and improves the finished product quality with almost the same cycle time obtained by low coolant temperature. As regards to coolant flow velocity effect, an optimum value of about 1 m.s$^{-1}$ improves part quality and provides a compromise between the cycle time and process profitability.

**Keywords:** RHCM process / cooling / split flow / operating parameters / profitability / modeling

## 1 Introduction

During the injection molding process, the mold temperature is of great importance since it affects the quality of the finished thermoplastic products. For the rapid heat cycle molding (RHCM) process, the mold is heated to a preset high temperature before each filling stage, then, the mold is cooled down to solidify the molten polymer for demolding. In order to successfully perform a RHCM operation, it is important to promote uniform a rapid heating/cooling providing the good product quality and the high RHCM process productivity.

Previous experimental studies [1–4] have shown the significance of the mold cavity surface temperature increase on the improvement of the finished products appearance and quality by avoiding the premature solidification of the molten polymer. Further, surface defects such as flow marks and weld lines can be eliminated. Recently, many previous works [5–7] have applied the RHCM process into the microcellular injection molding (MIM). These works have demonstrated the effectiveness of the RHCM process in the improvement of microcellular injected parts surface quality. Moreover, in the case of micro-injection, Felice and Roberto [8] have shown, when substituting conventional injection molding (CIM) by the RHCM process, that a significant increase in the flow length of the molten polymer was noticed. Therefore, with the RHCM process, the injections of micro thick and long parts are feasible.

Many previous works have mainly been focused on the optimization of the geometric and operating parameters of the RHCM process. In the field of design optimization, Wang et al. [9,10], based on the response surface methodology (RSM) and the multi-objective particle swarm optimization (MOPSO) algorithms, have developed a method to optimize the arrangement of heating/cooling channels. The used geometrical parameters [9,10] are the channel diameter, distance cavity-channel and the channel number. The optimal arrangement of heating/cooling channels leads to a 61.7% reduction of the heating time, a 80.9% attenuation in the temperature gap at the cavity surface, and a slight decrease in thermal stresses. Likewise, Wang et al. [11] have used two objective functions to optimize the heating/cooling channels layout for RHCM mold

* e-mail: fatmakria1984@yahoo.fr

producing air conditioning panel in order to provide the heating efficiency and the temperature distribution uniformity. They [11] have considered the spacing between channels and distance channels-cavity. An optimized arrangement of channels leads to an excellent panel appearance. Luca et al. [12] have developed and optimized the design of a porous insert to enhance the heat transfer between cooling water and cavity surface of the RHCM mold. With the optimized porous inserts, the finished surfaces of fiber-reinforced polymer have been improved and a maximum heating rate of 7 °C.s$^{-1}$ has been reached. Wang et al [13] have conducted a 3D numerical study of the first heating of an RHCM mold producing an automotive part. They [13] have compared an "original design" composed of horizontal straight channels and an "optimal design" including vertical channels with baffles. They [13] have demonstrated an improvement of 27.3% in the heating efficiency when changing the original design by the optimal configuration. More recently, Hammami et al. [14] and Kria et al. [15] have demonstrated, through 3D numerical thermal regulation studies of RHCM molds, the necessity of carrying out simulations of several heating/cooling cycles until reaching the regular regime since they have found a strong difference between the first cycle and the regular one. They [14–15] have shown that since the second heating/cooling cycle the regular regime is reached. Kria et al. [15] have further developed the thermal regulation system of complex shaped part and have [15] proposed a "new conformal design" of heating/cooling channels combining simple horizontal drillings with concentric vertical tubes. The proposed design gives homogeneous heat extracted from concave and convex areas of the complex shaped automotive part with a considerable reduction of the cycle time.

In conventional injection molding process, operating parameters studies involving the initial temperature of the polymer part and the cooling rate were conducted [16] to numerically demonstrate the interaction between crystallization rate and temporal thermal evolution of the mold. Furthermore, in RHCM process, heating/cooling operating techniques have aroused particular interest in previous works. For rapid mold heating, two methods have been used in anterior works: internal and external mold heating. For external mold heating methods, flame heating [17], induction heating [18] and infrared heating [19] have been proposed. In the case of internal heating method, the mold temperature increase is given either by a heating fluid (saturated steam, water, oil) [20] circling through the mold channels, or by an integrated electric heating [21] system. For rapid mold cooling, Wang et al. [20] have shown the effectiveness of water cooling in comparison with oil cooling. Besides, they [20] have carried out the mold material effect on RHCM process response, and they [20] have demonstrated that mold material with high thermal conductivity and low specific heat are more convenient for the RHCM process so as to ensure the process productivity. Furthermore, considering constant coolant temperatures during the cooling phase, Hammami et al. [22] have been interested in hot and cold mediums temperatures effect on the RHCM process efficiency. They [22] have revealed that increasing the saturated steam temperature promotes process productivity. In addition, they [22] have demonstrated that, with high cooling water temperature range (50–60 °C), the part quality and the process profitability have been improved with nearly the same productivity obtained with low cooling temperatures range (20–40 °C).

Previous works dealing with the operating parameters study of the RHCM process are still limited. Moreover, during the polymer part cooling, a simplified hypothesis which assumes a constant coolant temperature during its passage through the mold channels is often assumed, which limits the investigation of thermal behaviors at cavity/core plates and polymer domains. For these reasons, we propose, in this work, to carry out a parametric study by coupling three domains: cavity/core plates, polymer, and coolant. Considering the heating/cooling channels design with split flow, our study investigates the operating parameters effects during the cooling phase on the RHCM process efficiency. The involved parameters in our research work are the coolant temperature and flow velocity at the inlet of channels. In order to determine the effect of these parameters on the RHCM process efficiency, RHCM times, energy consumption, temperature gap at cavity functional surfaces and maximum temperature difference (MTD) were used. The efficiency of the RHCM process is obtained: on the one hand, by reducing the RHCM cycle time and the energy consumption, thus promoting the process productivity and profitability, and on the other hand, by minimizing the temperature gap and the MTD. Therefore homogeneous temperature distribution is obtained at cavity surfaces and at the automotive part, and thus, improving the finished product quality.

## 2 Mathematical formulation and numerical method

To analyze the geometric and operating parameters effect on the RHCM process efficiency, thermal behavior at entirely RHCM mold domains, covering cavity/core plates, polymer and coolant, was studied. The phenomenological equations describing thermal transfers at the different domains during the heating/cooling stages were described in this section. The studied article is a complex-shaped automotive part (Fig. 1a) made with PC typed LEXAN Resin 915R (Tab. 1) [23]. In order to promote part quality and RHCM process productivity, the copper alloy AMPCO 940 (Tab. 1) [24] was used as material of the cavity/core plates.

Initially, the mold temperature was assumed to the ambient temperature, equal to 30 °C. At the beginning of the RHCM process, the mold is rapidly heated by saturated steam at 180 °C until reaching a temperature equal to 140 °C, slightly higher than the glass transition temperature of the considered polymer at the functional cavity surface (which supplies the external automotive part surfaces). During the heating phase, the mold cavity is empty and the computational domain is limited to the cavity/core plates. At this domain, heat transfer is

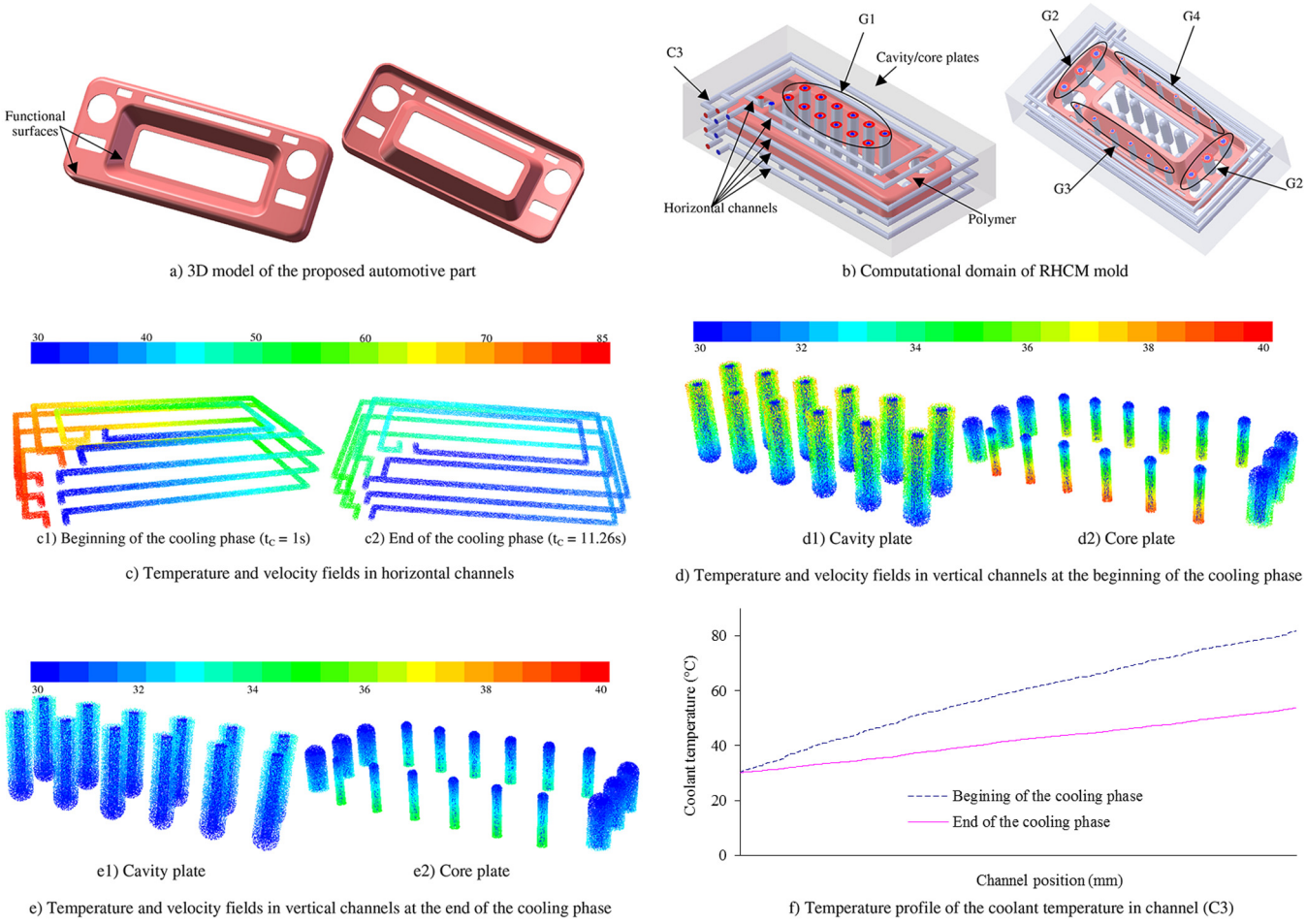


**Fig. 1.** First heating/cooling channels design. (a) 3D model of the proposed automotive part; (b) computational domain of RHCM mold; (c) temperature and velocity fields in horizontal channels; (d) temperature and velocity fields in vertical channels at the beginning of the cooling phase; (e) temperature and velocity fields in vertical channels at the end of the cooling phase; (f) temperature profile of the coolant temperature in channel (C3).

described by the conduction equation (1):

$$\rho_{\mathrm{m}} \quad C_{\mathrm{m}} \frac{\partial T_{\mathrm{m}}}{\partial t} = \frac{\partial}{\partial x_i} \quad \left( \lambda_{\mathrm{m}} \quad \frac{\partial T_m}{\partial x_i} \right). \tag{1}$$

At the mold plates-channels interface, heat transfer is given by conducto-convective equation (3):

$$\lambda_{\mathrm{m}} \quad \left( \frac{\partial T_{\mathrm{m}}}{\partial n_{\mathrm{m}}} \right)_{\text{channel}-\text{mold interface}} = h_{\mathrm{H}} \quad (T_{\mathrm{s}} - T_{\mathrm{m}})_{\text{channel}-\text{mold interface}}. \tag{2}$$

For vertical heating channels, convective heat transfer coefficient (3) is obtained from the Nusselt condensation theory for the laminar flow of a condensate film falling into a tube of height $L$ [25]:

$$h_{\mathrm{H\ vertical}} = 0.943 \left[ \frac{\lambda_{\mathrm{w}}^3 \rho_{\mathrm{w}} (\rho_{\mathrm{w}} - \rho_{\mathrm{s}}) g \mathrm{H}_{\mathrm{liq}}}{\mu_{\mathrm{w}} L (T_{\mathrm{s}} - T_{\mathrm{m}})_{\text{Channel}-\text{mold interface}}} \right]^{1/4}. \tag{3}$$

Rohsenow and Hartnett [25] derive a similar equation (4) for the condensation of a saturated liquid film on horizontal tubes giving a heat transfer coefficient in a horizontal tube of diameter $D$:

$$h_{\mathrm{H\ horizontal}} = 0.555 \left[ \frac{\lambda_{\mathrm{w}}^3 \rho_{\mathrm{w}} (\rho_{\mathrm{w}} - \rho_{\mathrm{s}}) g \mathrm{H}_{\mathrm{liq}}}{\mu_{\mathrm{w}} D (T_{\mathrm{s}} - T_{\mathrm{m}})_{\text{Channel}-\text{mold interface}}} \right]^{1/4}. \tag{4}$$

Assuming that the external surfaces of the cavity/core plate external are insulated, the thermal transfers to the ambient can be supposed to be negligible, so that the amount of energy required to heat the mold is calculated as follows:

$$Q_{\mathrm{consumed}} = \iiint_{\mathrm{mold}} \rho_{\mathrm{m}} C_{\mathrm{m}} \Delta T_{\mathrm{m}} \mathrm{d}v,$$

with $\mathrm{d}v$ the differential volume, $\Delta T$ is the difference between the temperatures of the mold at the end and at the beginning of the heating phase.

**Table 1.** Thermal properties of polymer [23] and mold plates [24].

| | Temperature (°C) | Density ($kg\,m^{-3}$) | Heat capacity ($J\,kg^{-1}\,K^{-1}$) | Thermal conductivity ($W\,m^{-1}\,K^{-1}$) |
|---|---|---|---|---|
| Mold material AMPCO 940 | | 8710 | 380 | 208 |
| Polymer PC typed LEXAN Resin 915R | 120 | 1190 | 1612 | 0.275 |
| | 130 | | 1693 | 0.278 |
| | 140 | | 1823 | 0.282 |
| | 150 | | 1885 | 0.286 |
| | 160 | | 1909 | 0.298 |
| | 170 | | 1929 | 0.31 |
| | 180 | | 1947 | 0.322 |
| | 200 | | 1976 | 0.227 |
| | 220 | | 2003 | 0.235 |
| | 240 | | 2020 | 0.242 |
| | 260 | | 2030 | 0.248 |

After heating the mold to the predetermined temperature, the mold cavity is assumed to be filled with the polymer at the injection temperature of 255 °C, and the cooling phase is instantly started. Then, it is assumed that the cavity/core plates' temperature distribution at the end of the heating phase provides the initial condition for the cooling phase.

During the cooling stage, thermal transfers in the mold (1) and polymer (5) domains are purely conductive. Take into account the phase change of the polymer during the cooling phase, the heat capacity of the polymer $C_p$ is considered as a function of the temperature.

$$\rho_{\mathrm{p}} \quad C_{\mathrm{p}}(\boldsymbol{T}_p)\frac{\partial T_{\mathrm{p}}}{\partial t} = \frac{\partial}{\partial x_i} \quad \left(\boldsymbol{\lambda}_{\mathrm{p}}(T_{\mathrm{p}}) \quad \frac{\partial T_{\mathrm{p}}}{\partial x_i}\right). \tag{5}$$

Take into consideration the temperature rise of the cooling fluid circling through the channels, the equations describing the heat transfer in cooling channels are fully coupled to the heat transfer equations governing thermal behavior in the mold and the polymer part.

The water flow through cooling channels occurs in the turbulent regime. The Reynolds-averaged Navier–Stokes equations (RANS equations) are time-averaged equations of motion for fluid flow. Thus, for steady incompressible flows, the continuity equation can be reduced to:

$$\frac{\partial V_i}{\partial x_i} = 0. \tag{6}$$

The time-averaged momentum equation can be written as follows:

$$\frac{\partial V_i}{\partial t} + V_j\frac{\partial V_i}{\partial x_j} + \frac{\partial \overline{v_i v_j}}{\partial x_j} = -\frac{1}{\rho}\frac{\partial P}{\partial x_i} + \frac{\partial}{\partial x_j}\left(\nu\frac{\partial V_i}{\partial x_j}\right). \tag{7}$$

Reynolds stresses are related to the mean flow via the Boussinesq hypothesis, so the time-averaged momentum equation can also be written as follows:

$$\frac{\partial V_i}{\partial t} + V_j\frac{\partial V_i}{\partial x_j} = -\frac{1}{\rho}\frac{\partial P}{\partial x_i} + \frac{\partial}{\partial x_j}\left((\nu+\nu_t)\frac{\partial V_i}{\partial x_j}\right). \tag{8}$$

The chosen turbulence model is the standard $k$-$\varepsilon$ model. In the $k$-$\varepsilon$ model, the effective or "turbulent" viscosity ($\nu_{\mathrm{t}}$) is computed from the turbulent kinetic energy "$k$" and the rate of dissipation of this energy "$\varepsilon$":

$$\nu_{\mathrm{t}} = C_\mu\frac{k^2}{\varepsilon}, \tag{9}$$

$k$ and $\varepsilon$ are predicted by the solution of their transport equations:

$$\frac{\partial k}{\partial \mathrm{t}} + V_i\frac{\partial k}{\partial x_i} = \frac{\partial}{\partial x_i}\left[\left(\nu+\frac{\nu_{\mathrm{t}}}{\sigma_k}\right)\frac{\partial k}{\partial x_i}\right] + \nu_{\mathrm{t}}\left(\frac{\partial V_j}{\partial x_i}+\frac{\partial V_i}{\partial x_j}\right)\frac{\partial V_j}{\partial x_i} - \varepsilon, \tag{10}$$

$$\frac{\partial \varepsilon}{\partial t} + V_i\frac{\partial \varepsilon}{\partial x_i} = \frac{\partial}{\partial x_i}\left[\left(\nu+\frac{\nu_t}{\sigma_\varepsilon}\right)\frac{\partial \varepsilon}{\partial x_i}\right] + \frac{\varepsilon}{k}\left[C_{\varepsilon 1}\nu_t\left(\frac{\partial V_j}{\partial x_i}+\frac{\partial V_i}{\partial x_j}\right)\frac{\partial V_j}{\partial x_i} - C_{\varepsilon 2}\varepsilon\right], \tag{11}$$

where the model constants are: $C_\mu = 0.09$; $C_{\varepsilon 1} = 1.44$; $C_{\varepsilon 2} = 1.92$; $\sigma_k = 1$, $\sigma_\varepsilon = 1.3$

The time-averaged temperature equation can be written as:

$$\rho_{\mathrm{w}}C_{\mathrm{w}}\left(\frac{\partial T}{\partial t} + V_i\frac{\partial T}{\partial x_i}\right) = \frac{\partial}{\partial x_i}\left((\lambda+\lambda_t)\frac{\partial T}{\partial x_i}\right). \tag{12}$$

**Table 2.** Geometric characteristics of vertical channels.

| | Main diameter (mm) | Outer tube diameter (mm) | Main drilling length (mm) | Number |
|---|---|---|---|---|
| G1 | 12 | 6 | 44 | 12 |
| G2 | 14 | 7 | 32 | 6 |
| G3 | 8 | 5 | 34 | 6 |
| G4 | 6 | 4 | 32 | 6 |

The distribution of eddy heat conductivity is then evaluated by applying Reynolds analogy:

$$\lambda_t = \frac{C_W \mu_t}{Pr_t}. \quad (13)$$

The cooling stage finishes when the polymer in the whole cavity is cooled to 120 °C. At this moment, the mold is opened and the part is ejected. In this study, the additional times (mold opening and closing and part ejection) are neglected. It is then supposed that just at the end of the cooling phase, the heating stage for the next cycle begins. Thus, our work is limited to the study of a succession of heating/cooling cycles during the RHCM process.

The meshing of the computational domain was conducted using the preprocessor GAMBIT 2.3.16 and the resolution of the established equations was carried out using the commercial code Fluent 6.3.26. The solver "pressure based implicit formulation" in the cyclic transient regime was used to determine the thermal behavior in the various domains as well as the hydrodynamic behavior in the coolant domain. Pressure-velocity coupling is achieved by using SIMPLE algorithm. With reference to spatial and temporal discretization, the second-order upwind scheme and the implicit scheme were, respectively, used.

## 3 Results and discussion

In order to analyze the influence of heating/cooling channels design and the operating parameters effects on the process efficiency, RHCM times (heating, cooling, and cycle) and consumed energy were chosen as criteria for assessing productivity and profitability. Furthermore, temperature gap on cavity plate functional surfaces after heating and MTD in the polymer domain after part cooling were selected as criteria for estimating part quality.

### 3.1 Effect of heating/cooling channels design on RHCM process efficiency

#### 3.1.1 First design of heating/cooling channels

In order to regulate the temperature of RHCM mold producing a complex shaped automotive part (Fig. 1a), a first design of heating/cooling channels is proposed as shown in Figure 1b. The adopted arrangement of heating/cooling channels has recently been studied and proved to be efficient for the RHCM process (Kria et al. [15]). In addition to horizontal channels, circumventing the automotive part shape, the thermal control system includes vertical channels to access to convex zones in cavity/core plates in order to enhance heat transfer in these regions during the RHCM process.

Figure 1b exhibits the computational domains involving cavity/core plates, polymer, and heating/cooling channels. The fluid domain (heating/cooling channels) includes five horizontal channels with 6 mm in diameter, and four groups of vertical channels whose geometrical characteristics are listed in Table 2. A mesh comprising 4328063 tetrahedral elements (2767787 elements in mold domain, 855008 elements in polymer domain and 705268 in coolant domain) and a time step of $10^{-3}$ s were proved necessary and sufficient to have precise results in a minimum computational time.

Using a cooling water temperature of 30 °C and a flow velocity of 2 m.s$^{-1}$ at the inlet of channels, the simulation of several heating/cooling cycles during the RHCM process was undertaken until reaching a cyclic regular regime.

Figures 1c–1e show the velocity and the temperature fields in horizontal and vertical channels at the beginning ($t_C = 1$ s) and at the end ($t_C = 11.26$ s) of the cooling phase.

In Figure 1c, giving temperature and velocity fields in horizontal channels, it can be seen that the coolant temperature sensibly increases along its path through the channels. Particularly, a significant rise in the temperature takes place along the longer channels. It is noted that at $t_C = 1$ s, the temperature at the outlet of the longest channel (800 mm) is 83 °C, while, for the shortest channel (535 mm), the temperature is 71.4 °C. With regard to vertical channels (Figs. 1d and 1e), it can be seen that the cooling water temperature remains unchanged when running through the inner tubes and then increases progressively in the annular space.

By comparing the coolant temperature increase between the beginning and the end of the cooling stage, a significant drop of the longitudinal temperature profiles along the channels at the end of the cooling stage can be observed (Fig. 1f). Particularly, the mean temperature at horizontal channels outlet decreases from 80 °C at the beginning of the cooling phase to 51.5 °C towards the end of this stage. This can be explained by the fact that the mean mold temperature is high enough (139 °C) at the beginning of the cooling phase, and then decreases to 81.5 °C at the end of the cycle.

With the first heating/cooling channels design, a significant increase in the cooling water temperature was found along its path through the RHCM mold, which consequently leads to non-homogeneous cooling polymer conditions. To overcome this disadvantage, a second design of channels was proposed to reduce the coolant path.

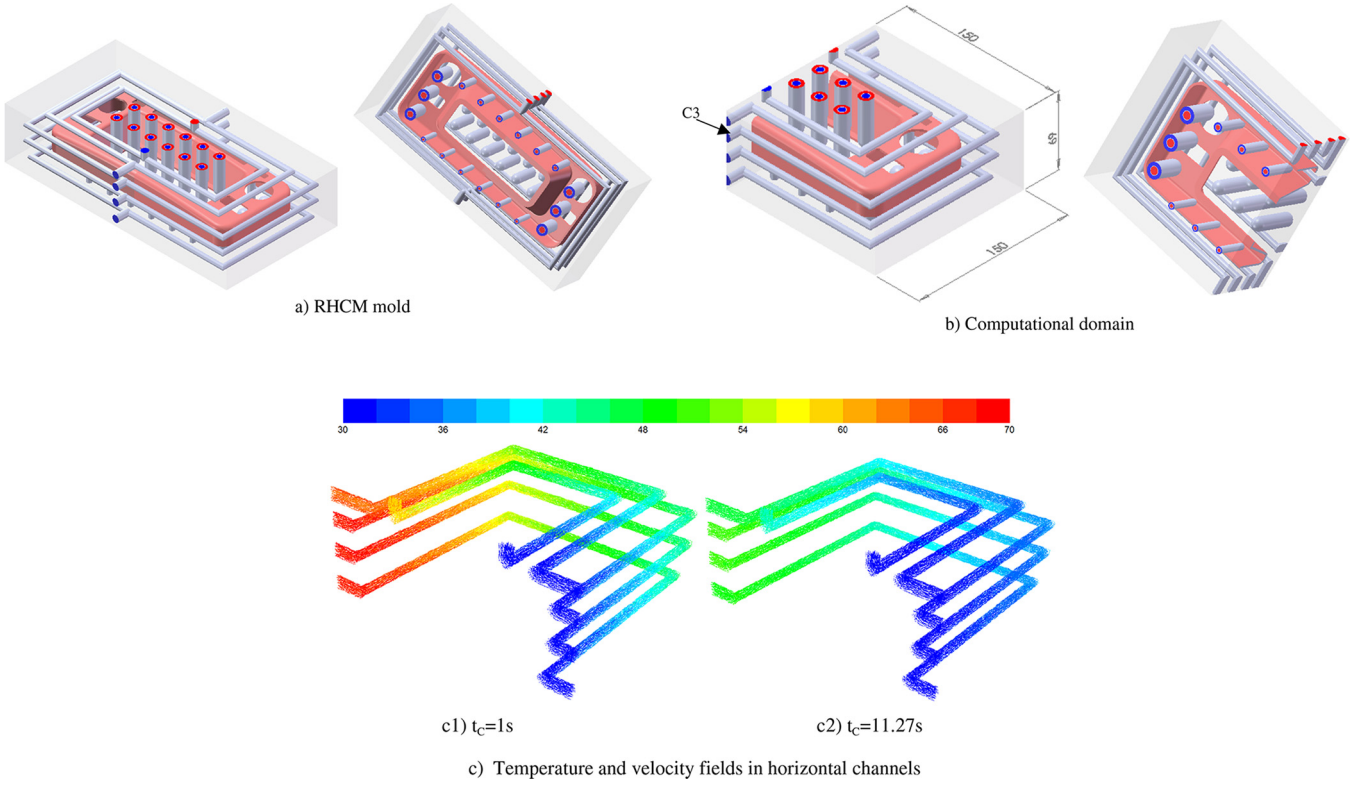


**Fig. 2.** Heating/cooling channels with split flow design. (a) RHCM mold; (b) computational domain; (c) temperature and velocity fields in horizontal channels.

### 3.1.2 Second design: heating/cooling channels with coolant split flow

Figure 2a displays the RHCM mold with the second channels design. For the proposed solution, the design of vertical channels is maintained while the design of horizontal channels is improved by imposing a split flow configuration. The cooling water stream bifurcates in two currents to be engaged in horizontal channels circumventing the automotive part on both sides. By adopting, in the entrance of the channels, the same adopted mass flow rate imposed in the first design, the simulation of several heating/cooling cycles was carried out.

Considering the symmetries, the computational domain could be limited to $\frac{1}{2}$ RHCM mold (Fig. 2b). At the mold symmetry plane, a zero heat flux condition was applied. For this design, computational domain includes 2163973 tetrahedral elements distributed as follows: 1383851 elements in mold domain, 427488 elements in cavity/core plates' domain, and 352634 elements in coolant domain.

The velocity field and temperature distribution in horizontal channels obtained after attaining the regular cyclic regime are illustrated in Figure 2c in two cases: at the beginning ($t_C = 1$ s) and at the end of the cooling phase ($t_C = 11.27$ s). It can be clearly seen that the temperature rise of coolant at the beginning of the cooling stage ($t_C = 1$ s) is more significant than the temperature increase obtained at the end of the cooling stage ($t_C = 11.27$ s). Particularly, the mean temperature at $t_C = 1$ s at the outlet of the horizontal channels is about 65 °C, whereas, at $t_C = 11.27$ s, the average temperature at the channels outlet is equal to 47.9 °C.

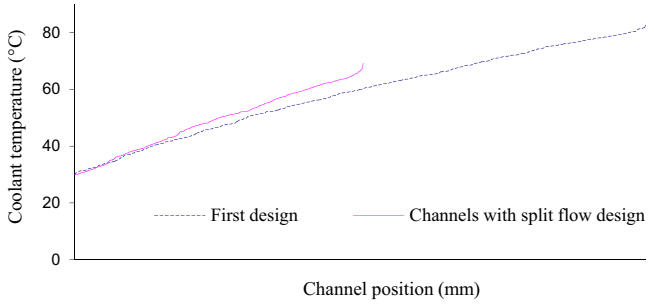


**Fig. 3.** Longitudinal profile of coolant temperature in channel (C3) at $t_C = 1$ s.

Since the total mass flow rate, imposed by the first design, was equally split into two networks of channels, therefore the same coolant residence time was saved. Figure 3, giving the longitudinal temperature profile on the channel (C3) at $t_C = 1$ s, shows slightly higher levels of temperature with the split-flow configuration. However, the temperature in the outlet of channel (C3) corresponding to split-flow design is substantially lower than that obtained with the first design (68 °C compared to 83 °C). The main reason can be attributed to the reduction of the heat transfer coefficient which depends on the coolant velocity.

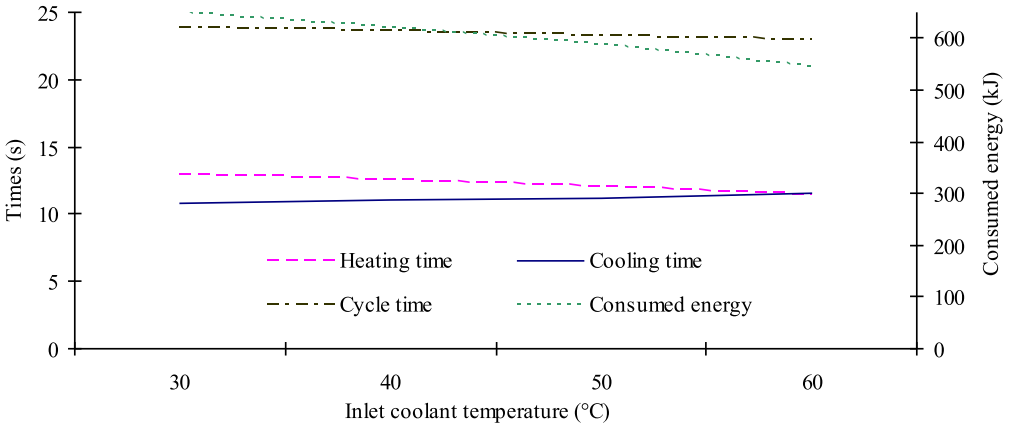


a) RHCM times and consumed energy

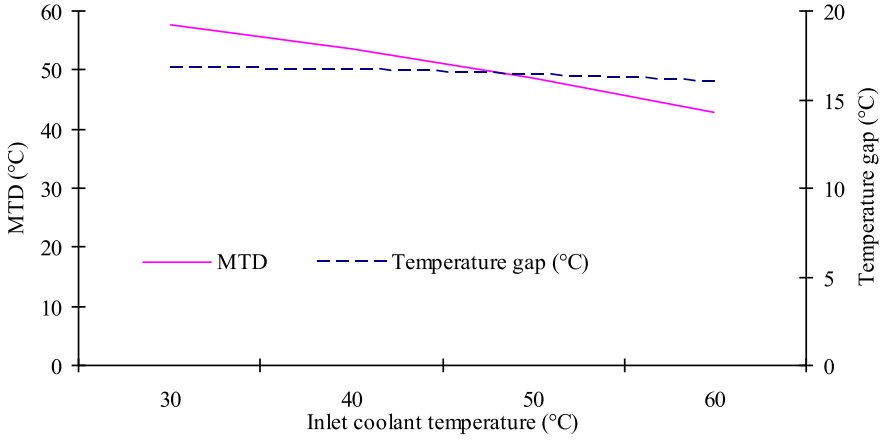


b) M.T.D and temperature gap

**Fig. 4.** Effect of the cooling water temperature. (a) RHCM times and consumed energy; (b) MTD and temperature gap.

#### 3.1.3 Comparison between the two proposed channel designs

By comparing the two channel configurations, we highlight that the cooling time remains almost constant ($t_C = 11.26$ s for the first design and $t_C = 11.27$ s for the second design). However, with the second split flow design, the outlet coolant temperatures are lower, i.e., the evacuated energy by the coolant is less important: 545.5 kJ against 608.3 kJ corresponding to the first design.

Furthermore, the heating time slightly decreases (12.4 s against 11.68 s with the second design). Thereby, with the second design, the profitability was improved by reducing the energy consumption while the RHCM process productivity was maintained.

With respect to the finished product quality, the used indicators for this purpose show a positive tendency. The temperatures' gaps at cavity plate functional surfaces are 18 and 16.1 °C obtained, respectively, with the first and second design. As for the MTD, it varies from 51.3 °C for the first design to 45.4 °C in the second design. This can be explained by the fact that the second shorter channels design supplies more homogeneous temperature fields.

Subsequently, it can be concluded that the second design of heating/cooling channels promotes RHCM process quality and profitability, without affecting the process productivity. Proceeding with the second design, the following section will be devoted to the operating parameters study, namely the coolant temperature and coolant flow velocity at the inlet of horizontal and vertical channels, during the cooling stage of the RHCM process.

### 3.2 Effect of the operating parameters

#### 3.2.1 Effect of the cooling water temperature

In order to analyze the cooling water temperature effect on the RHCM process evolution, different inlet temperatures (30, 40, 50 and 60 °C) with a constant flow velocity of 2 m.s$^{-1}$ were tested. Figure 4a presents the effect of cooling water temperature on the RHCM times as well as on the consumed energy. It can be seen that the increasing of the coolant temperature raises slightly the cooling time (6.5%) and decreases the heating time (12%) resulting in an almost constant cycle time (the overall cycle times difference does not exceed 3%). In fact, the increase of the cooling water temperature contributes to a reduction of driving force for

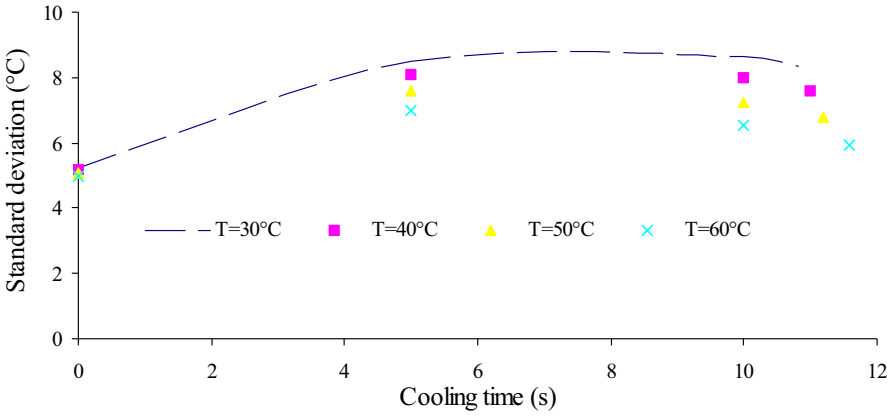


**Fig. 5.** Variation of the temperature standard deviation at cavity surface during the cooling phase.

heat transfer, which is temperature difference between the mold and the flowing cooling water in channels, and consequently, the increase of the cooling time.

On the other hand, the coolant temperature decrease contributes to a slight reduction of the cooling time, but to a much more significant decrease in cavity/core plates' temperature. Thus, an unnecessary undercooling is obtained at mold plates, which slows down the mold heating and requires supplying a larger quantity of heat to reach the adequate temperature at the cavity functional surfaces. This explains an increase of 16% in the consumed energy by reducing channels inlet temperature from 60 to 30 °C.

In order to investigate the cooling water temperature effect on the finished product quality, the variation of the temperature gap as well as the MTD as a function of coolant temperatures (Fig. 4b) was analyzed. It can be seen that, for the temperature range of (30–60 °C), the coolant temperature increase has a little effect (4%) on the temperature gap at cavity plate functional surfaces. However, the increase in coolant temperature reduces the MTD by 26%. To account for this tendency, Figure 5 provides the standard deviation of cavity surfaces temperature during the cooling stage for the different considered coolant temperatures. It can be noted that the temperature standard deviation gradually decreases with the coolant temperature increase. As a direct consequence, the cooling process of the automotive part gives rise to a better temperature homogenization and presents the weakest MTD for a cooling water inlet at 60 °C.

To conclude, we can say that the process productivity is not affected for the temperature range 30 to 60 °C. However, an increase of the cooling water temperature provides improvements in RHCM process profitability and part quality.

### 3.2.2 Effect of the cooling water flow velocity

In this section, the cooling water flow velocity effect on the RHCM process efficiency was investigated. Three flow velocities ($V=1\,\mathrm{m.s^{-1}}$, $V=1.5\,\mathrm{m.s^{-1}}$ and $V=2\,\mathrm{m.s^{-1}}$) were tested, and in each case, different coolant temperatures ($T=30\,°\mathrm{C}$, $T=40\,°\mathrm{C}$, $T=50\,°\mathrm{C}$, $T=60\,°\mathrm{C}$) at the inlet of horizontal and vertical channels were considered.

Taking into account a fixed channels inlet temperature of 40 °C, Figure 6 shows, at $t_C=1\,\mathrm{s}$, a general overview of the velocity and temperature fields at horizontal channels for the different proposed flow velocities. It can be observed that the coolant temperature gradually increases along its path through the channels, and the increase in temperature is more pronounced at low flow velocity ($V=1\,\mathrm{m.s^{-1}}$). For $V=2\,\mathrm{m.s^{-1}}$, the mean temperature at the outlet of horizontal channels is of 69.15 °C, whereas, for $V=1\,\mathrm{m.s^{-1}}$, the average temperature is about 75.3 °C. In fact, the increase of the coolant flow velocity promotes the heat exchange as a result of the rise of convective heat transfers at the channels-mold plates' interfaces. However, the flow velocity increase reduces the residence time of the cooling water inside the channels which increases the driving force for heat transfer.

Figures 7a–7d display histograms supplying the variation of the RHCM times and the consumed energy as a function of the cooling water temperature for different flow velocities. The histograms presented in Figure 7a reveal, in the studied temperature range (30–60 °C), that the increasing of the coolant flow velocity accelerates the automotive part cooling. It is noteworthy that a decrease of 18% in cooling time when changing the flow velocity from $V=1\,\mathrm{m.s^{-1}}$ to $V=2\,\mathrm{m.s^{-1}}$, regardless of the inlet coolant temperature, occurs. The reduction in the RHCM time can be chiefly explained by the decrease of heat transfer resistance at the coolant–mold interface with the increase of the coolant flow velocity. During the cooling stage, the studied domain can be subdivided into three thermal resistances in series: a first convective thermal resistance situated at the channels surfaces (mold plates-coolant), a second conductive resistance ascribed to the cavity/core plates domain and a third conductive resistance corresponding to the polymer domain which manifests the highest thermal resistance attributed to the low conductivity of the polymer.

The cooling water velocity increase acts directly on the resistance at the channels interface, which yields enhancing heat transfers. Consequently, at the end of the cooling phase, the mold plates domain has an average temperature of 86.3 °C for $V=2\,\mathrm{m.s^{-1}}$ and 96 °C for $V=1\,\mathrm{m.s^{-1}}$.

The effect of the coolant velocity and temperature inlet on the heating phase is illustrated by the histograms reported in Figure 7b. As it can be shown, an increase in the

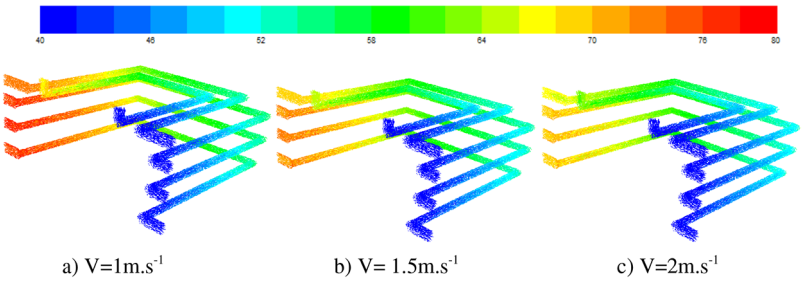


**Fig. 6.** Velocity and temperature fields at horizontal channels at $t_C = 1$ s. (a) $V = 1\,\mathrm{m.s^{-1}}$; (b) $V = 1.5\,\mathrm{m.s^{-1}}$; (c) $V = 2\,\mathrm{m.s^{-1}}$.

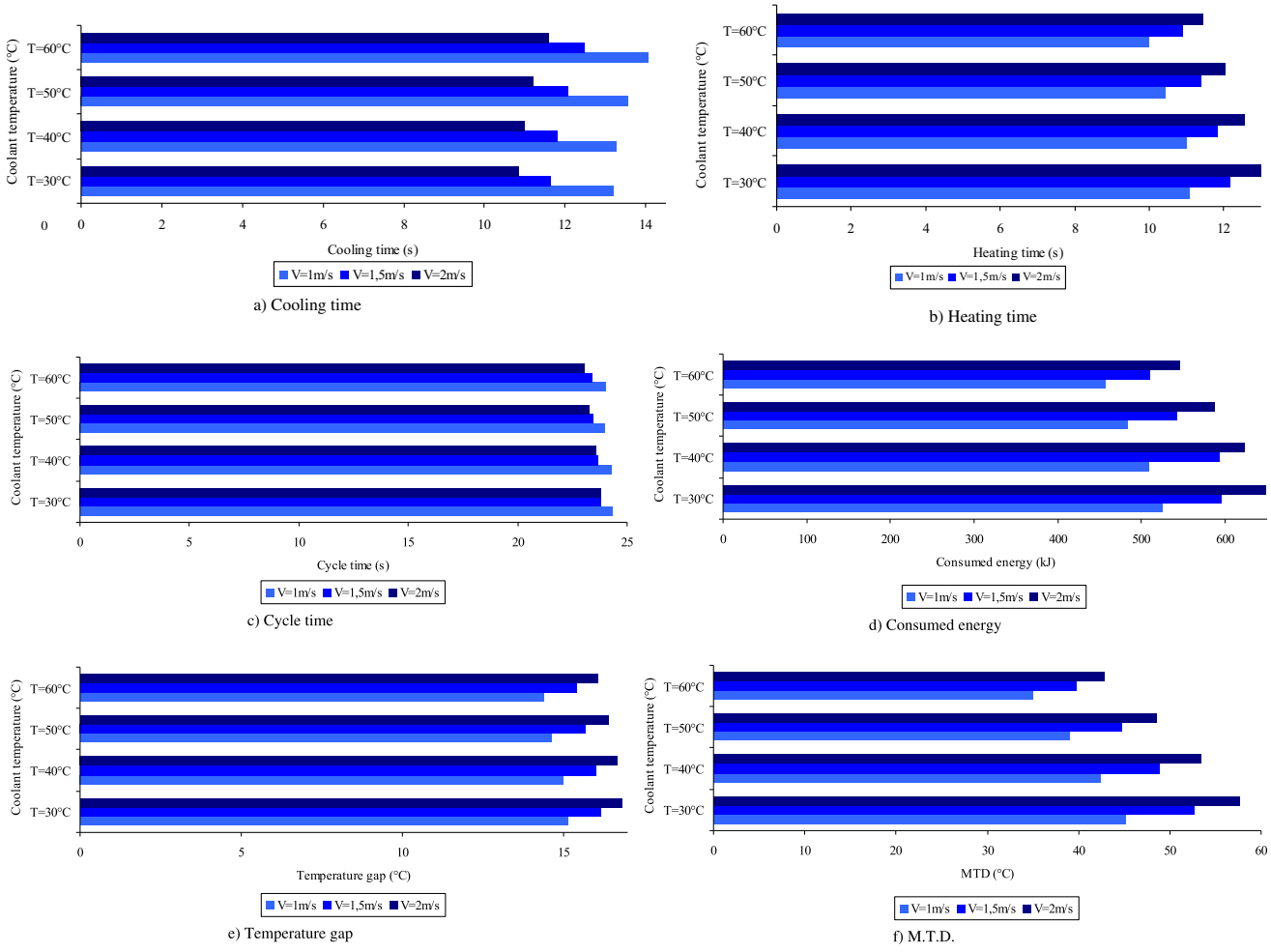


**Fig. 7.** Effect of the cooling water flow velocity for different coolant temperature. (a) Cooling time; (b) heating time; (c) cycle time; (d) consumed energy; (e) temperature gap; (f) MTD.

heating time is caused by the increase of the cooling water velocity and the decrease of the water inlet temperature, which leads to an undercooling of the cavity/core plates.

As a result of the total cycle time, the acceleration of the cooling phase followed by a slowdown of the heating phase leads to an almost constant cycle time (maximum deviation of 4%) (Fig. 7c).

Furthermore, an increase in the consumed energy with the increase of cooling water flow velocity was detected (Fig. 7d). This increase is more expressed for a coolant temperature of 30 °C. For example, the energy consumption increases by 19% when coolant flow velocity changes from 1 to 2 $\mathrm{m.s^{-1}}$. Since at the end of the heating phase the average temperature of the mold plates is almost the same (145 °C), the energy consumption increase is mainly related to an under cooling of the cavity/core plates.

The efficiency of the RHCM process is related to the productivity as well as the quality of the finished product. The temperature gap and the MTD are retained as criteria to quantify the product quality. The histograms represented in Figure 7e display a little variation in the temperature gap at the cavity plate functional surfaces for

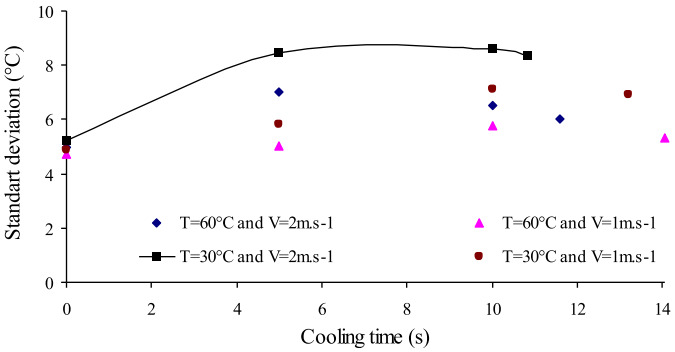


**Fig. 8.** Variation of the thermal standard deviation during the cooling stage.

the different considered coolant velocities. This trend is reproduced for the temperature range (30–60 °C). As for the MTD, it can be seen that an increase in the coolant flow velocity increases the thermal gradients at the finished product (Fig. 7f), and this increase is more important as the temperature of the cooling water is low. Considering the cooling process at $T = 30$ °C, the MTD was increased by about 27%, whereas, a cooling with a temperature of 60 °C leads to a rise of only 18%.

In order to account for the flow velocity effect on the MTD, the standard deviations of the cavity surfaces temperature, which are in direct contact with the automotive article during the cooling phase, were retained as criteria (Fig. 8). It can be noted, at the beginning of the cooling phase, that the temperature standard deviations are almost the same. Subsequently, the temperature distributions, just at the beginning of the cooling stage have the same homogeneity. Subsequently, as the mold is cooled, a heterogeneity of the temperature fields is observed at the cavity surface. This trend is more pronounced for low water temperatures (30 °C) and high coolant velocity inlet.

## 4 Conclusion

In this work, the thermal behavior of RHCM mold for complex shaped automotive part production was investigated. Particularly, the effect of the operating parameters, namely the cooling water temperature and flow velocity, on the RHCM process productivity and the finished product quality, were analyzed. In order to determine the operating parameters effect on the RHCM process efficiency, four parameters were selected: the cycle time and the consumed energy that reflects the productivity and profitability effect, together with the temperature gap as well as the MTD that reveals the impact on the finished product quality.

Using the commercial software Fluent 6.3.23, numerical simulations of thermal behavior in mold plates, polymer and coolant domain during several heating/cooling cycles were conducted. A reduction of about 50% in the cycle time and in the consumed energy since the second heating/cooling cycle was demonstrated. However, the cooling time was kept almost constant from the first cycle. Moreover, it is shown that, by maintaining a constant mass flow rate of cooling water, the heating/cooling channels with split flow design promotes process profitability while maintaining almost the same level of process quality and productivity.

Concerning the operating parameters effect on the RHCM process with split flow design, the following conclusions can be drawn:

- the reduction of the cooling water temperature accelerates the mold cooling and slows down the heating process while at the same time maintains an almost constant cycle time;
- although the coolant temperature has no importance on the productivity process, the water temperature increase reduces the energy consumption, the MTD and, slightly the temperature gap. Based on these results, it may be concluded that a coolant temperature of 60 °C at the inlet of channels promotes the RHCM profitability and products quality;
- regarding the cooling water flow velocity effect, it was demonstrated that a flow velocity of 2 $m.s^{-1}$ accelerates the cooling, decelerates the heating so as to maintain an almost constant cycle time. However, an increase in the consumed energy, MTD as well as the temperature gap was noted;
- to achieve a successful RHCM operation, it was proved that a coolant temperature of 60 °C flowing at 1 $m.s^{-1}$ is the most suitable operating parameter to ensure the RHCM process productivity, profitability, and automobile part quality.

## Nomenclature

| | |
|---|---|
| $C$ | Heat capacity ($J\,kg^{-1}\,K^{-1}$) |
| $T$ | Temperature (°C) |
| $t$ | Time (s) |
| $n$ | Normal direction |
| $h$ | Heat transfer coefficient ($W\,m^{-2}\,K^{-1}$) |
| $g$ | Gravity acceleration ($m\,s^{-2}$) |
| $H_{liq}$ | Liquefaction latent heat of water ($J\,kg^{-1}$) |
| $L$ | Channel height (m) |
| $D$ | Channel diameter (m) |
| $V$ | Average velocity ($m\,s^{-1}$) |
| $v$ | Fluctuating velocity ($m\,s^{-1}$) |
| $P$ | Pressure (Pa) |
| $k$ | Turbulent kinetic energy ($m^2\,s^{-2}$) |

## Greek symbols

| | |
|---|---|
| $\rho$ | Density ($kg\,m^{-3}$) |
| $\lambda$ | Thermal conductivity ($W\,m^{-1}\,K^{-1}$) |
| $\mu$ | Dynamic viscosity ($kg\,m^{-1}\,s^{-1}$) |
| $\nu$ | Kinetic viscosity ($m^2 s{-}1$) |
| $\varepsilon$ | Turbulent kinetic energy dissipation rate ($m^2\,s^{-3}$) |

## Dimensionless number

Pr Prandtl number

## Subscripts

m Mold
s Saturated steam
H Heating
p Polymer
t Turbulent
g Glass transition
w Water
c Cooling

## References


[1] G. Wang, G. Zhao, Y. Guan, Thermal response of an electric heating rapid cycle molding mold and its effect on surface appearance and tensile strength of the molded part, J. Appl. Polym. Sci. 128 (2013) 1339–1352

[2] G. Wang, G. Zhao, X. Wang, Experimental research on the effects of cavity surface temperature on surface appearance properties of the molded part in rapid heat cycle molding process, Int. J. Adv. Manuf. Technol. 68 (2013) 1293–1310

[3] G. Lucchetta, M. Fiorotto, P.F. Bariani, Influence of rapid mold temperature variation on surface topography replication and appearance of injection-molded parts, CIRP Ann. Manuf. Technol. 61 (2012) 539–542

[4] G. Lucchetta, M. Fiorotto, Influence of rapid mould temperature variation on the appearance of injection moulded parts, J. Mech. Eng. 59 (2013) 683–688

[5] Cheng-Long Xiao, Han-Xiong Huang, Xing Yang, Development and application of rapid thermal cycling molding with electric heating for improving surface quality of microcellular injection molded parts, Appl. Therm. Eng. 100 (2016) 478–489

[6] Lei Zhang, Guoqun Zhao, Guilong Wang, Guiwei Dong, Hao Wu, Investigation on bubble morphological evolution and plastic part surface quality of microcellular injection molding process based on a multiphase-solid coupled heat transfer model, Int. J. Heat Mass Transf. 104 (2017) 1246–1258

[7] Lei Zhang, Guoqun Zhao, Guilong Wang, Formation mechanism of porous structure in plastic parts injected by microcellular injection molding technology with variable mold temperature, Appl. Therm. Eng. 114 (2017) 484–497

[8] Felice De Santis, Roberto Pantani, Development of a rapid surface temperature variation system and application to micro-injection molding, J. Mater. Process. Technol. 237 (2016) 1–11

[9] G. Wang, G. Zhao, H. Li, Y. Guan, Multi-objective optimization design of the heating/cooling channels of the steam-heating rapid thermal response mold using particle swarm optimization, Int. J. Therm. Sci. 50 (2011) 790–802

[10] G. Wang, G. Zhao, H. Li, Y. Guan, Research on optimization design of the heating/cooling channels for rapid heat cycle molding based on response surface methodology and constrained particle swarm optimization, Expert Syst. Appl. 38 (2011) 6705–6719

[11] M.H. Wang, J.J. Dong, W.H. Wang, J. Zhou, Z. Dai, X.R. Zhuang, Optimal design of medium channels for water-assisted rapid thermal cycle mold using multiobjective evolutionary algorithm and multi-attribute decision-making method, Int. J. Adv. Manuf. Technol. 68 (2013) 9–12

[12] Luca Crema, Marco Sorgato, Giovanni Lucchetta, Thermal optimization of deterministic porous mold inserts for rapid heat cycle molding, Int. J. Heat Mass Transf. 109 (2017) 462–469

[13] G. Wang, G. Zhao, X. Wang, Heating/cooling channels design for an automotive interior part and its evaluation in rapid heat cycle molding, Mater. Des. 59 (2014) 310–322

[14] Moez Hammami, Fatma Kria, Mounir Baccar, Numerical study of thermal control system for rapid heat cycle injection molding process, Proc. Inst. Mech. Eng., Part E: J. Process Mech. Eng. 229 (2015) 315–326

[15] Fatma Kria, Moez Hammami, Mounir Baccar, Conformal heating/cooling channels design in rapid heat cycle molding process, Mechanics and Industry 18 (2017) 109

[16] M'hamed Boutaous, Nadia Brahmia, Patrick Bourgin, Parametric study of the crystallization kinetics of a semi-crystalline polymer during cooling, Comptes rendus mecanique 338 (2010) 78–84

[17] D.H. Kim, M.H. Kang, Y.H. Chun, Development of a new injection molding technology: Momentary mold surface heating process, J. Inject. Molding Technol. 5 (2001) 229–232

[18] K. Park, S.I. Lee, Localized mold heating with the aid of selective induction for injection molding of high aspect ratio micro-features, J. Micromech. Microeng. 20 (2010) 1–11

[19] M.C. Yu, W.B. Young, P.M. Hsu, Micro-injection molding with the infrared assisted mold heating system, Mater. Sci. Eng.: A 460–461 (2007) 288–295

[20] G. Wang, G. Zhao, H. Li, Y. Guan, Analysis of thermal cycling efficiency and optimal design of heating/cooling systems for rapid heat cycle injection molding process, Mater. Des. 31 (2010) 3426–3441

[21 G. Wang, G. Zhao, H. Li, Y. Guan, Research of thermal response simulation and mold structure optimization for rapid heat cycle molding processes, respectively, with steam heating and electric heating, Mater. Des. 31 (2010) 382–395

[22] M. Hammami, F. Kria, M. Baccar, Numerical study of the operating parameter effect on rapid heat cycle molding process, Proc. Inst. Mech. Eng., Part E: J. Process Mech. Eng. 231 (2017) 1075–1084

[23] Autodesk simulation Moldflow adviser, (2014)

[24] Moldflow plastic insight release, 5.0 (2002)

[25] M.W. Rohsenow, J.P. Hartnett, Handbook of heat transfer, McGraw-Hill, New York, 1973


**Cite this article as**: F. Kria, M. Hammami, M. Baccar, A modeling study on the effect of operating parameters on RHCM process using split flow channels design, Mechanics & Industry **20**, 503 (2019)